Original Research
ISSN (Print): 0971-6580
ISSN (Online): 0976-5131
Journal of Endocrinology and Reproduction, *Vol 25(1), 37-49, June 2021, DOI: 10.18311/jer/2021/27986*

Peptidyl Arginine Deiminase 2 (PADI2) is Expressed in Post-Meiotic Germ Cells in the Mouse Testis and is Localized Heavily on the Acrosomal Region of Spermatozoa

Mahitha Sahadevan[1,2] and Pradeep G. Kumar[1*]

[1]Division of Molecular Reproduction, Rajiv Gandhi Centre for Biotechnology, Thycaud PO, Poojappura, Thiruvananthapuram – 695014, Kerala, India
[2]Department of Biotechnology, University of Kerala, Kariavattom, Thiruvananthapuram – 695034, Kerala, India; kumarp@rgcb.res.in

Abstract

Peptidyl Arginine Deiminase 2 (PADI2) is a widely expressed Ca^{2+} ion-dependent enzyme in rodents and humans belonging to Peptidyl Arginine Deiminases (PAD) family. It regulates various cellular processes like proliferation, differentiation, apoptosis, migration, epithelial-mesenchymal transition and chromatin organization. Altered expression of PADI2 was associated with various autoimmune diseases, neurological disorders and different types of cancers. Based on our previously published miRNA-mRNA network during the first wave of spermatogenesis in the mouse, *Padi2* appeared to be a common potential target of miR-34c and miR-449a in the mouse testes. In the present study, the expression of *Padi2* in the mouse testes during the first wave of spermatogenesis was evaluated using real-time PCR, western blot analysis and immunohistochemistry. Transcript levels of *Padi2* showed progressive down-regulation during the first wave of spermatogenesis. However, we detected a progressive increase in the levels of PADI2 as the first wave of spermatogenesis progressed, with heavy expression of this protein in post-meiotic germ cells. Additionally, a prominent localization of PADI2 in the acrosomal region of late spermatids and spermatozoa was identified through immunohistochemical analysis. *Padi2* expression was identified in germ cell-derived cell lines, C18-4 and GC-1 spg as well. Thus, the present study illustrates for the first time the expression of PADI2 in germ cells in the testis and its predominant localization on the acrosome region of spermatozoa, suggesting its potential role in fertilization.

Keywords: Gene Expression, Peptidyl Arginine Deiminase 2, Spermatogonia, Spermatogenesis, Testis

1. Introduction

Spermatozoa are specially designed haploid cells formed as the result of a well-orchestrated process called spermatogenesis, packed with crucially needed organelles to accomplish its function of fertilizing the ovum. Before fertilization, the spermatozoon and the oocyte undergo several progressive biochemical and molecular changes in a precise and orderly manner which is prerequisite for the successive fusion of gametes[1-5]. Previous studies have documented the drastic remodelling of cytoskeleton and cellular organelles during the transformational journey of immotile spermatogonial mother cell to form a motile sperm[6-13]. The spermatozoa possess a specialized structure known as acrosome, which is a highly conserved unique membrane-bound organelle positioned over the anterior region of sperm nucleus[14-16]. The acrosome carries numerous hydrolytic/proteolytic enzymes in the

*Author for correspondence

molecular scaffolds of the acrosomal matrix, which helps the sperm to penetrate the zona pellucida and finally bind to the oolemma of the egg. Defects in the structure or function of acrosome lead to impaired sperm fusion, which eventually results in male infertility[17-21]. It has also been reported that even a point mutation in the vesicular protein (Vps54) involved in acrosomogenesis results in impaired spermatogenesis[22,23]. Absence of the acrosomal matrix component Zona Pellucida-Binding Protein 1 (ZPBP1) or 2 (ZPBP2) results in acrosomal dysplasia[18]. *In vitro* fertilization using intra-cytoplasmic sperm injection failed when the spermatozoon carrying acrosomal abnormalities was used, due to its inefficiency in activating the oocyte[24-28] Understanding the molecular defects of the spermatozoa associated with their functional incompetence would be important to manage male factor infertility and also to develop contraceptives in future[29-31].

As spermatozoa are transcriptionally and translationally inactive, the proteins they possess are either expressed before *de novo* gene expression is silenced in the germ cells during the progression of spermatogenesis or are acquired from the surroundings during their transit through the male reproductive tract. The first wave of spermatogenesis is an excellent phase to profile the temporal expression profiles of genes during germ cell differentiation at the time of spermatogenesis. A previous study from our lab had reported dynamic alterations in the miRNA-mRNA networks during the first wave of spermatogenesis in mouse. Progressive upregulation of miR-34c and miR-449a appeared to be critical in initiating the germ cell differentiation events in the testis[32]. These two miRNAs belong to the same family of miRNAs. Several predicted targets of these miRNAs were mined out from a transcriptome dataset generated in our laboratory[32]. Peptidyl Arginine Deiminase 2 (*Padi2*) gene is one of the predicted common targets of miR-34c and miR-449a[32]. As PADI2 has been shown to be involved in cell differentiation and chromatin reorganisation, we evaluated the expression of *Padi2* during the first wave of spermatogenesis using postnatal 8, 16, and 24 day mouse testes. The observed localization of PADI2 on the acrosomal region of late spermatids and spermatozoa is suggestive of its possible role in fertilization.

2. Material and Methods

2.1 Experimental Animals

Swiss albino male mice of four age groups - postnatal day 8 (P8), 16 (P16), 24 (P24) and adult (AD, three month old) were obtained from an inbred line maintained in the institute animal house facility to check the expression of gene on the onset of spermatogenesis. Animals were reared in temperature (26 ±1˚C) and humidity-controlled environment under 14h light: 10h dark conditions. Use of experimental animals for this study was approved by the Institutional Animal Ethics Committee (IAEC), Permit Nos. IAEC/219/PKG/2015 & IAEC/289/PRK/2015, Rajiv Gandhi Centre for Biotechnology, Thiruvananthapuram.

2.2 Reagents

DMEM, DMEM/F-12, FBS, antibiotic–antimycotic solution, MEM Non-Essential Amino acids solution (Invitrogen, Green Island, CA); miRNeasy Mini kit (Qiagen, Hilden, Germany); SuperScript® VILO™ cDNA synthesis kit (Invitrogen, Waltham, MA); dNTPs, 100bp ladder, Taq polymerase (New England Biolabs, Ipswich, MA); Taq DNA Polymerase from Thermusaquaticus (Sigma, St. Louis, Mo, USA); PCR primer (Sigma Genosys, Bangalore, India); SYBR green master mix, MicroAmp™ Optical 384-Well Reaction Plate with Barcode, MicroAmp™ Optical Adhesive Film (Applied Bio systems, Waltham, MA), HybondTM-P PVDF membrane (GE Healthcare, NA, UK); PADI2 antibody (Abcam, Cambridge, United Kingdom); β-actin, goat anti-rabbit HRP, donkey anti-goat HRP, primary and secondary antibody (Santa Cruz Biotechnology, Dallas, TX) were procured; DAPI (4′,6-diamidino-2-phenylindole), Alexa fluor 488 - conjugated goat anti-rabbit Ig G, ProLong™ Diamond Antifade Mountant (Thermo Fisher Scientific, MA, USA); GC1-spg cell line (CRL:2053) (ATCC, VA, USA); Skimmed milkpowder (Sagar, India); Agarose, Acrylamide, APS, BSA, bis-acrylamide, Boric acid, Chloroform, Critic acid, DAB, EGTA, EDTA, Ethidium bromide, Glycine, Glycerol, KH_2PO_4, 2-mercaptoethanol N,N,N',N'-tetramethylethylenediamine, Na_2HPO_4, Nickel chloride, Paraformaldehyde Potassium chloride, Protease Inhibitor cocktail, Phenyl Methane Sulphonyl Fluoride (PMSF), SDS, Trizma Base, Triton X 100, Tween 20, Sodium deoxycholate, Sodium Citrate, Sodium chloride (Sigma Aldrich, MO,USA), Bromophenol blue(SR

Laboratories,India); Ethanol and Methanol (Merck, USA), Hydrogen peroxide and Hydrochloric acid (SD Fine chemicals, India); Bouin'sfixative (Polysciences, Inc. Warrington, USA); Starfrost microscopic slides (Knittelglass, Germany), Xylene (Thermo Fisher Scientific, Mumbai, India) and Surgipath Paraplast High Melt (Leica, Mount Waverley, The Netherlands) were used in this study.

2.3 Cell Culture

GC1-spg and C18-4 cells were cultured in 25 cm^2 cultured flasks containing complete growth medium comprised of Dulbecco's Modified Eagle's Medium (DMEM) and DMEM F12 with 1 % non-essential amino acid (NEAA), respectively, supplemented with 10 % FBS and 1 % antibiotic–antimycotic. The cells were incubated at 37° C in an incubator maintaining 5 % CO_2. The cells were harvested for RNA isolation once the cells reached 95 % confluence.

2.4 RT-PCR

Total RNA was isolated from one pair of postnatal day 8, 16 and 24 mouse testes per preparation using the miRNeasy kit (Qiagen). Tunica albuginea was removed before proceeding with RNA isolation, followed by homogenizing the tissue for 3 min using PLYTRON PT –ST 2101 homogenizer (Kinematica, Luzernerstrasse, Germany) by adding 700 µL QIAzol lysis reagent. Further, total RNA was isolated as per the miRNeasy kit manufacturer's protocol. In case of cell lines (C18-4 and GC-1 spg), the RNA was isolated, once the cells reached 95 % confluence using the same kit as per the manufacturer's protocol. The resulting RNA was quantified using NanoDrop TM 1000 (Thermo Scientific, DE, USA) and 1 µg RNA was reverse transcribed using SuperScript™ VILO™ cDNA synthesis kit as per the manufacturer's protocol. *Padi2* and *β-Actin* primers were designed using NCBI Primer-BLAST (sequences of primers listed in Table 1). Total volume of 22 µL PCR reaction was set up by adding 1 µL cDNA, 2.5 µL Taq polymerase buffer containing 1.5 mM $MgCl_2$, 0.20 mM dNTP mix (1 µL), 0.5 units (0.5 µL) of Taq polymerase, 1 µM each of forward and reverse primers (1 µL) and 15 µL MilliQ water in an Applied Biosystems Verti thermal cycler under standard PCR condition. PCR products were run in 2 % agarose gel, and the images were captured using VersaDoc MP4000 gel documentation system and the Quantity One software (Bio-Rad Laboratories, CA, USA). *Beta actin* gene expression was taken as internal control. The experiment was performed using three biological replicates.

2.5 Real-time PCR

RNA was extracted from one pair of mouse testes from each age group, using miRNeasy kit (Qiagen) and cDNA were transcribed using the SuperScript™ VILO™ cDNA

Table 1. Details of primer used for RT-PCR and real-time PCR analysis

Sl. No.	Gene	Primer sequence 5'-3'	Length of target fragment (bp)	Function
1.	*Padi2* F	CCGAGAAAAGCAGAAGGCAG	484	RT-PCR
2.	*Padi2* R	GTGCCACCACTTGAAGGTGA		
3.	*β-Actin F*	TCTGATGGTGGGAATGGGTCAG	500	RT-PCR
4.	*β-Actin R*	TTTGATGTCACGCACGATT		
5.	*Gapdh* F	CCAGCTACTCGCGGCTTTA	145	Real-time PCR
6.	*Gapdh* R	GAGGGCTGCAGTCCGTATTT		
7.	*Padi2* F	AGATGATCCTGCGCACCAAA	122	Real-time PCR
8.	*Padi2* R	GCCAAAGAACGGGTTCTCCA		

synthesis kit as mentioned above. Further, the cDNA was diluted ten times before proceeding to real-time PCR by adding RNase-free water. PCR was done using specific forward and reverse primers of *Padi2* (sequences of primers listed in Table 1) in a total of 5 µL reaction with SYBR green master mix in ABI 7900 HT Sequence Detection System (Applied Biosystems, Netherlands) under standard qPCR temperature conditions. The following cycling parameters were used: 50° C for 10 min, 90° C for 10 min, and 95° C for 10 minutes. This was followed by 40 cycles of 95° C for 10 s and a combined annealing/extension temperature of 60° C for 2 min. Expression level of *Gapdh* was used as internal control. Three biological replicates, each with three technical replicates and with appropriate controls including no template controls (NTCs) were analysed. The relative fold changes were calculated in other age groups with respect to P8 mouse testes and mean ΔΔCt values were used to plot the graph. Statistical analysis was performed using Paired two tailed Student *t*-test between the age groups, viz., P8 *vs* P16 and P16 *vs* P24 as represented by asterisk on the histogram.

2.6 Immunoblotting

Total testicular protein was extracted from five biological replicates using RIPA buffer containing 10 µL of 100 mM Tris-HCl (pH 7.5), 140 µL of 140 mM NaCl, 2 µL of 1 mMEDTA, 1 µL of 0.5 mM EGTA, 10 µL of 1 % Triton, 100 µL of 0.1% sodium deoxycholate, 10 µL of 1 mM phenyl methyl sulfonyl fluoride, 717 µL dd H2O and 10 µL 1x protein inhibitor cocktail (HY-K0010, MCE). The tissue was disrupted by using POLYTRON PT–ST 2101 homogenizer (Kinematica, Luzernerstrasse, Germany) for 2 min in RIPA buffer. The lysate was kept in rotospin at a speed of 50 x g in cold room for 30 minutes for agitation, followed by centrifugation at 4° C at 10,000 x g and the supernatant was collected. Protein concentration was determined using Quick Start™ Bradford 1x Dye reagent (Bio-Rad, Hercules, CA). 40 µg of protein sample was resolved on a 12 % polyacrylamide gel, followed by overnight electrophoretic transfer to a PVDF membrane using a BioRad Mini TransBlot cell (BioRad, Hercules, CA). The membrane was blocked using 5 % milk in PBS containing 0.1 % Tween 20 (PBST) for 1 hour at room temperature followed by three PBST washes before adding anti-PADI2 antibody (ab50257, 2:1000 dilution in PBST) for overnight incubation at 4° C. Further, horseradish peroxidase (HRP)-conjugated goat anti-rabbit antibody (sc-2030, 1:2000 dilution in PBST) was used as the secondary antibody and was incubated for 1 hour at room temperature before developing the blot using a solution containing 0.1 % $NiCl_2$, 0.05 % DAB, and H_2O_2. The images were captured using the VersaDoc Gel Documentation system and the Quantity One Software (Bio-Rad Laboratories, CA, USA) and band intensities were quantified using Image Lab TM Software Version 4.1. Mouse β-ACTIN (sc-1616) was used as loading control. Secondary antibody used for probing was rabbit anti-goat (1:2000, sc-2768).The protein expression was compared with P8 *vs* P16, P16 *vs* P24 and P24 *vs* adult and the significances were calculated using two tailed Student's *t*- test.

2.7 Immunohistochemistry and Immunofluorescence

Whole testes were fixed in Bouin's fluid overnight at room temperature. The tissues were dehydrated using ascending order of ethanol series (50 %, 75 %, 90 % and 100 %), cleared in xylene and embedded in paraffin. Testes sections of 0.5 µm thicknesses were prepared and deparaffinized in xylene, followed by passing them through a descending order of ethanol series (100 %, 90 %, 70 %, and 50 %) and final washing using distilled water before antigen retrieval step. Antigen retrieval was performed by microwaving the sections for 10 min in citrate buffer (pH 6). In case of immunocytochemistry**,** the mouse spermatozoa were collected from the caudal segment of epididymis and fixed using freshly prepared 4 % paraformaldehyde. Further cells were premeabilized using 0.1 % Triton. Both testes tissues sections and spermatozoa were blocked using 5 % goat serum for 1 hour at room temperature in a humidified chamber, before incubating with primary antibody anti-PADI2 (ab50257, 1:200 in 1 % BSA) for overnight at 4° C, which was further incubated with Alexa fluor 488-conjugated secondary antibody (1:400 in 1 % BSA) for 1 hr at room temperature in the dark. In between each above said steps, slides were washed thrice with PBST to reduce background noise. Finally the nuclei of the cells were counter-stained using DAPI and slides were mounted using antifademountant (Prolong™ Diamond antifade mountant, P36970). The images were obtained using Leica TCS-SP2 Confocal Microscope equipped with AOBS system (Leica, Mannheim, Germany).

3. Results

3.1 RT-PCR and Real-Time PCR of *Padi2* in Mouse Testis during the First Wave of Spermatogenesis

Currently, little is known about the *Padi2* expression dynamics in the testis during the postnatal development of mouse. Therefore, the transcript level of *Padi2* during the onset of first wave of spermatogenesis was initially checked. The *Padi2* transcript levels in mouse testes of different postnatal days were confirmed using gene-specific internal primers which amplified the region between the exon 13 and 16, resulting in a 484 base pair amplicon. Among the three age groups selected in the study, *Padi2* transcript was highly expressed in postnatal day 8 testes, followed by a progressive decline in the transcript level as it progress from transition stage P8 *vs* P16 *vs* P24 (Figure 1A). Further, the relative expression fold change of *Padi2* was analyzed by real-time PCR. A similar pattern of gene expression was observed, as *Padi2* was highly expressed in P8 mouse testes, whereas there was four-fold reduction in the transcript level of *Padi2* in P24 testes (Figure 1B).

3.2 Western Blot Analysis of PADI2 in Mouse Testis During the First Wave of Spermatogenesis

PADI2 levels in the mouse testes were determined to check how the progressive reduction observed at the transcript level of this gene correlated with its protein levels. For this purpose protein was isolated from mouse testes of corresponding age groups similar to the time points chosen for transcript level study. Surprisingly, the western blot analysis showed a strong negative correlation of PADI2 expression levels with its mRNA levels (Figure 1C). Higher expression of PADI2 was observed at P16 and P24 when compared with P8 testes. The increase in

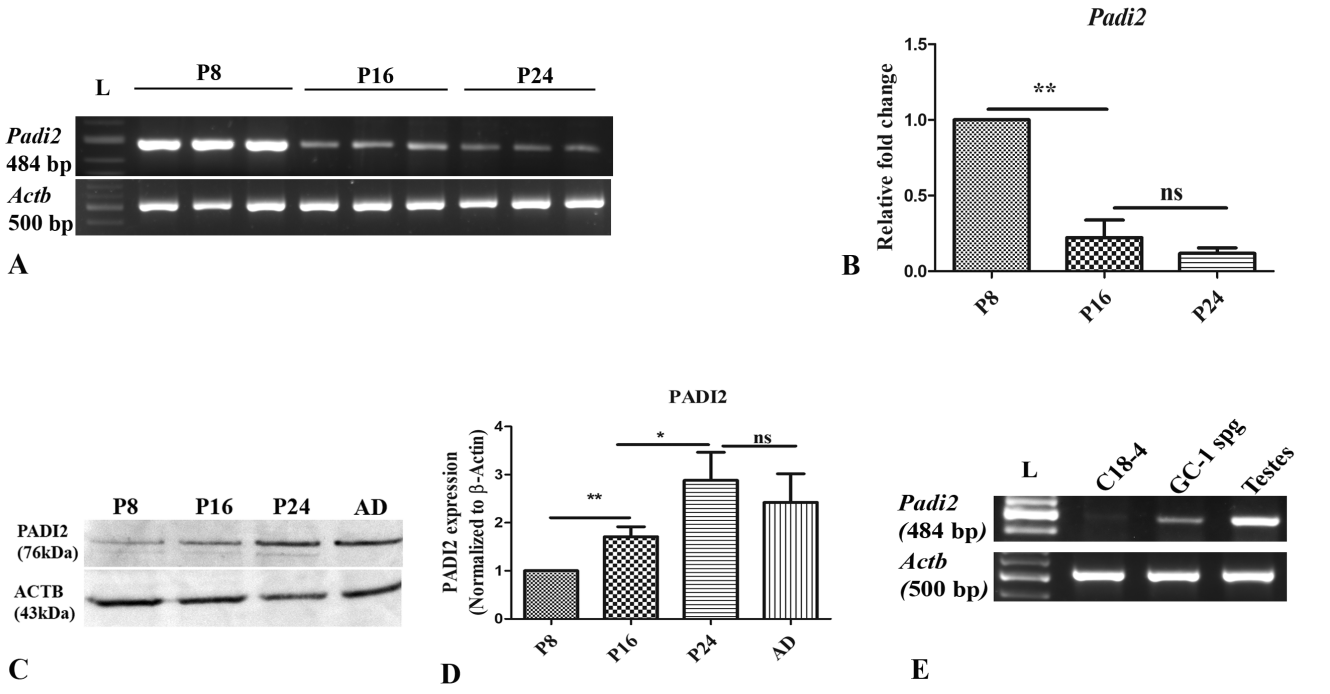

(A) Representative image of RT-PCR showing *Padi2* transcript level expression in the postnatal day 8 (P8), 16 (P16) and 24 (P24) mouse testis. *β-Actin* was used as endogenous control. Each lane represents different biological replicates. (B). Relative fold change of *Padi2*. AverageΔΔCt value obtained from three biological replicates was plotted in graph. *Gapdh* was taken as endogenous control.(C) & (D) Representative images of immunoblot analysis of PADI2 in various mouse age group testis P8, P16, P24 and AD (3 month old adult testes) and respective band intensity calculated using Image lab software, plotted in histogram (n=5).β-ACTIN was used as loading control. (E) Representative image of endogenous expression of *Padi2* in germ cell lines (C18-4 and GC-1 spg). Mouse testis (8 day, P8) was used as positive control. Significant difference between various age groups was calculated using Student's t-test. Asterisks indicate levels of statistical significance (***p<0.001, **p<0.01, *p<0.05, ns- not significant). L- 100 bp ladder.

Figure 1. *Padi2* expression in various age group mouse testis.

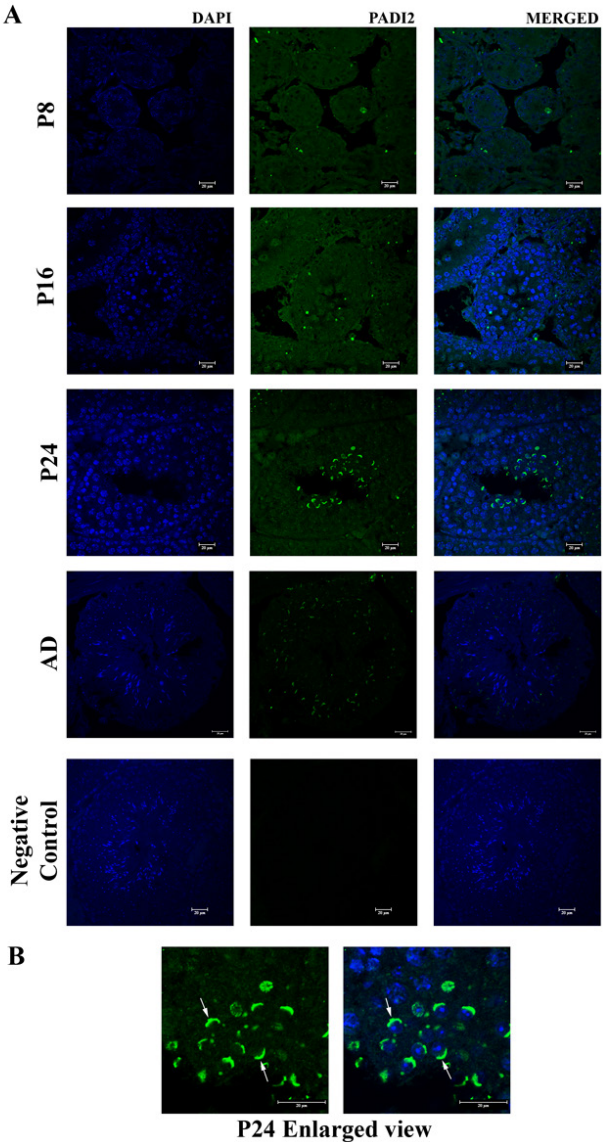

(A) Immunolocalization of PADI2 in postnatal day 8 (P8), 16 (P16) 24 (P24) and adult (AD) mouse testes and negative control. Weak and diffuse PADI2 expression was noted in both the somatic and germ cell of the testes at P8 and P16, with prominent localization observed in prospective acrosomal region of late spermatid at 24. Testes tissue sections were probed with anti-PADI2 (green fluorescent signal, using Alexa 488 secondary antibody) and nuclei were stained with DAPI. (B) A portion of PAD12 stained postnatal 24 mouse testes (enlarged view). The white arrow illustrates spermatids with robust PAD12 staining in the prospective acrosomal region.

Figure 2. Immunohistochemical analysis ofPADI2 in various age group mouse testes.

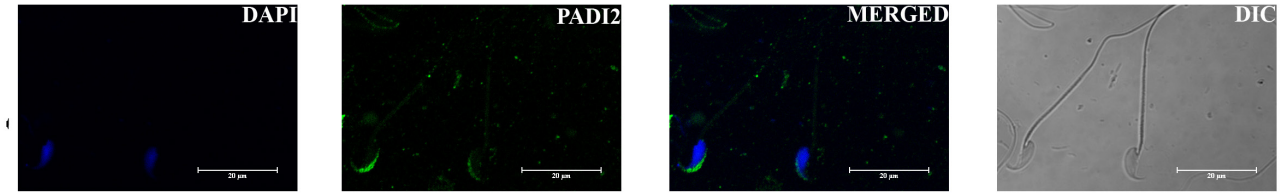

Cauda epididymal sperm were collected and probed using anti-PADI2 antibody, followed by detection using Alexa 488 conjugated secondary antibody (green fluorescent signal). Nuclei were counterstained using DAPI (blue). A prominent localization was observed near the acrosome region of sperm. Scale bar 20μm.

Figure 3. PADI2 localization in mouse spermatozoa.

the levels of PADI2 from P8 to P16 was highly significant ($p<0.01$) and that during P16 to P24 transition was also significant ($p<0.05$), as represented in the histogram showing the average of the band intensities computed from the five biological replicates (Figure 1D). The levels of PADI2 protein expression in the testes were maintained at its high levels as the animal entered into adulthood. Thus, it was identified that PADI2 levels in the testes showed a progressive up-regulation during the first wave of spermatogenesis, even though its transcript levels were progressively down regulated.

3.3 Immunolocalization of PADI2 in Mouse Testis

The localization of PADI2 in mouse testes during the different stages of the first wave of spermatogenesis was evaluated using immunofluorescence microscopy. PADI2 showed a weak and diffuse expression in all the cell types during the P8 and P16 stages. However, in the P24 and adult testes, it was predominantly found in the post-meiotic germ cells (Figure 2A). In P24 testes, an intense localization of PADI2 was noted in the developing acrosome of round and elongated spermatids, as can be clearly visualized at higher magnification (Figure 2B). The enrichment of PADI2 in the acrosome was observed in adult testes as well.

3.4 Immunolocalization of PADI2 on Spermatozoa

To verify if PADI2 localized heavily on the acrosome region of the spermatozoa in the testis is retained during the subsequent post-testicular maturational changes in the epididymis, we performed immunofluorescence localization of this molecule on spermatozoa are covered from the cauda epididymis of adult mouse. Our results indicated that PADI2 was retained on the acrosome region of the sperm head even after the completion of their epididymal maturation (Figure 3). A prominent and clear crescent-shaped localization pattern of PADI2 was observed in the acrosome region of sperm, consistent with the pattern observed in the spermatids, while a highly diffused and faint pattern were observed in its tail region.

3.5 Expression of *Padi2* in Immortalized Spermatogonial Cell Lines

It has been previously reported that *Padi2* was expressed exclusively in fetal Sertoli cells (33). However, our results demonstrated that germ cells expressed PADI2 and that its expression peaked up in post-meiotic germ cells in the mouse testis. To reconfirm *Padi2* expression in spermatogonial cells, we evaluated its expression in spermatogonial cell lines C18-4 and GC-1 spg by RT-PCR. Both these cell lines expressed *Padi2*, with higher expression observed in GC-1 spg compared to C18-4 cells (Figure 1E).

4. Discussion

In the present study, both the transcript and protein levels of *Padi2,* a tissue-specific sulfhydryl enzyme, which is now known as cysteine hydrolase, were analysed on the onset of first wave of spermatogenesis[34-36]. Postnatal days 8, 16 and 24 were selected mainly due to the stage-dependent enrichment of pre-meiotic, meiotic and post meiotic cells at these three stages in the mouse testis. Earlier studies have reported prominent distribution of PADI2 in the central nervous system, spleen, skeletal muscle, uterus, pancreas, skin, sweat gland, breast and leukocytes, whereas only a few sporadic reports are available regarding the presence of PADI2 in testes[33,34,37-44].

PADI2 is a ubiquitously expressed post-translational modifying sulfhydryl enzyme belonging to PADs family, which catalyses the citrullization process in protein in a calcium-dependent manner[39,45]. In rodents, four isoforms of PADI namely, PADI1, PADI2, PADI3 and PADI4 were identified based on differences in their molecular weights and tissue localization[45-48]. Christophorou *et al.* had previously reported that *Padi4* gene is a part of the pluripotency transcriptional network, which regulates the activation of key stem cell genes[49]. PADI2 regulates many cellular and biological process like chromatin organization, histone and protein citrullination, angiogenesis, oligodendrocyte differentiation, macrophage apoptosis, proliferation, cell migration and epithelial-mesenchymal transition[45,48-58]. Altered expression of PADI2 was shown in several pathological conditions including rheumatoid

arthritis, multiple sclerosis, psoriasis, chronic obstructive pulmonary disease and various cancers like breast cancer, epithelial bladder cancer, spontaneous skin tumors, colon cancer, and prostate cancer[47,50,54,55,58-66]. In cancer, PADI2 exhibits a tissue-specific role in mediating tumor progression. For instance, overexpression of PADI2 was linked with tumor progression in case of spontaneous skin neoplastia, whereas its down-regulation led to colon cancer[47,67,68]. Although the functions of this molecule were well documented in normal and pathological conditions in various tissues, it's possible roles in testicular biology and functional development of spermatozoa have not yet been elucidated.

Roger *et al.* had first described PADs enzyme responsible for post-translational modification (peptidyl-arginine to peptidyl-citrulline) in trichohyalin protein, which in turn is essential for hair growth[35]. In normal physiological condition, PADI2 remains in inactive form until stimulated with calcium. Once it is activated, it initiates citrullination of its target proteins[36]. Further, it has been reported that stimulated PADI2 can citrullinate a number of structural (e.g., vimentin, and keratin) and histone (e.g., H1, H2A, H3 and H4) proteins which modulate various cellular processes through regulating the gene expression[36,49,69-71]. Likewise, a plethora of studies has associated the dysregulation of *Padi2* in various autoimmune, inflammatory and neurological disorders like rheumatoid arthritis, multiple sclerosis, Alzheimer's disease and multiple types of cancers[34,36,37, 41,47,50,55,61-66,68,72-75].

In testes, Hosokawa *et al.* had reported the expression of *Padi2* exclusively in foetal Sertoli cells and that its expression was positively regulated by SOX9[33]. However, in the present study using immunofluorescence microscopy of mouse testis during three critical stages of the first wave of spermatogenesis, we have detected PADI2 expression in the germ cells as well. Further, we could also demonstrate *Padi2* expression in GC-1 spg and C18-4 cells, which are immortal cell lines, derived from type B and type A spermatogonial cells, respectively.

Padi2 was reported to be a common predicted target of miR-34c and miR-449a during the onset of the first wave of spermatogenesis in mouse testis[32]. Our real-time PCR analysis confirmed our previous microarray results which indicated a progressive down-regulation of the transcript levels of *Padi2* during the progression of the 1st wave of spermatogenesis in mouse testis. However, the levels of PADI2 showed a strong negative correlation (r = -0.7) with reference to the transcript levels (refer to the data display). This discrepancy observed in the transcript and protein levels could be due to factors including extended transcript stability, high translation efficiency, and low rate of protein degradation due to certain structural modification in protein structure based on cellular condition[76-82]. Moritz *et al.,* had reported poor correlation between transcript and protein in neuronal cells due to variations in protein transport[79].

Dong *et al.,* reported high expression of PADI isoform in terminally differentiated keratinocytes, associating it with the regulation of differentiation events[83]. Likewise, Falcao *et al.,* reported its chromatin modifier role in oligodendrocyte differentiation by regulating the expression of myelin gene. Moreover, its knockdown has been reported to diminish the differentiation of oligodendrocytes[45]. In addition, PADI2 helps in T helper (Th) cell differentiation by specifically citrullinating key transcription factors essential for Th cell functions such as GATA3 (arginine 330) and RORtγ (arginine 4)[84,85]. In the present study, PADI2 expression was found to be dramatically elevated in postnatal testes containing large number of differentiating germ cells. The predominant localization of PADI2 on the principal acrosomal domains of late spermatids and spermatozoa revealed compartmentalization of PADI2 in germ cells at later stages of their developmental sequence.

Among PADs isoforms, only PADI4 is known to have canonical Nuclear Localization Signal (NLS)[41,50]. However, recent studies had highlighted the presence of PADI2 in the nuclei of mammary epithelial cells and oligodendrocytes precursor cells[45,50]. Zheng *et al.,* had revealed that binding of calcium to PADI2 is the trigger for its translocation from cytoplasm to the nucleus by switching its binding from annex in 5 to the RanGTPase[86]. Various studies have reported the role of PADI2 in modulating numerous signalling pathways by regulating the chromatin organisation and key gene expression by releasing the pausing barrier of RNA polymerase II (RNAP2) close to the transcription start site, by citrullinating arginine1810 at the Carboxyl-Terminal Domain (CTD) of the largest subunit[87]. Wang *et al.* had reported its role in protein stability, nuclear translocation and transcriptional activation of androgen receptor in castration-resistant prostate cancer[66]. Liu *et al.* had documented the role of PADI2 in JAK2/STAT3 pathwayin A2780 and SKOV3 cells through mediating phosphorylation of STAT3 and regulating EMT (55). Like-wise, its role in regulating Wnt (wingless)/ β-catenin

signalling pathway was reported in colorectal cancer and was linked with poor prognosis[88].

The localization of PADI2 on spermatozoa is of special significance. In our understanding, this is the first report demonstrating the localization of PADI2 on the acrosomal domains of spermatozoa. The membrane system of the principal acrosomal domain of spermatozoa is subject to a host of calcium-dependent physicochemical modifications, and several molecules located in this domain have critical roles in mediating events leading to fertilization and activation of the oocyte. It is also a known fact that the spermatozoa undergo drastic molecular changes in the female reproductive tract through calcium-depended processes such as capacitation and acrosome reaction, which are prerequisites for fertilizing the ovum. The fact that calcium is essential for activating PADI2 and that it is specifically localized in the acrosome region of sperm point to its possible role in fertilization events. Notably, PADI4-mediated citrullination of histone H1 creates an open chromatin state of regulator genes, which in turn regulates stem cell pluripotency during early embryogenesis[87,89]. In addition, histone H3 and H4 citrullination on mitotic metaphase chromatin were observed in preimplantation embryos, which emphasize its role in chromatin condensation or decondensation[50,57]. Remarkably, the role of PADI2 in maintaining naive pluripotency by suppressing heterochromatin formation through H3Cit26 associates with SWI/SNF-related matrix-associated actin-dependent regulator of chromatin subfamily A proteins harboring DEAD/H box 1 domain[90]. Moreover, a recent study revealed that only PADI2, among all the members of PADs family, can citrullinate arginine1810 (Cit1810) in RNAP2, which enables the efficient transcription of genes involved in cell cycle progression, metabolism, and cell proliferation[87]. On the other hand, depleted PADI2 leads to inhibition of cell proliferation by suppressing the expression of MYC gene[50,87]. The depletion of PADI2 in mammary carcinoma led to mesenchymal to epithelial-like transition by supressing cytoskeletal regulatory proteins like RhoA, Rac1, and Cdc42[58]. Thus, the possibility of sperm-derived PADI2 playing a role in oocyte-zygote transition cannot be neglected.

In conclusion, this report, for the first time, documents the progressive increase in the expression of PADI2 during the 1st wave of spermatogenesis in mouse testis, despite the gradual decline of *Padi2* during this event. The localization of PADI2 on the acrosomal domain of late spermatids and mature spermatozoa is suggestive of its role in mediating the events associated with fertilization. In the light of earlier reports on the role of PADI family members during early embryogenesis, the role of sperm-derived PADI2 in oocyte-zygote transition demands further investigation.

5. Acknowledgments

PGK was supported by Grant No. BT/PR3600/MED/31/299/2015 from Department of Biotechnology, Government of India, and Intramural Research Funds from Rajiv Gandhi Centre for Biotechnology, Thiruvananthapuram. MS received a fellowship from University Grants Commission (UGC), Government. of India (Ref. No: 23/12/2012(ii)EU-V). The authors thank Jiji V and Gopikrishnan K for assistance in confocal microscopic imaging.

6. References

1. Bianchi E, Wright GJ. Find and fuse: Unsolved mysteries in sperm-egg recognition. PLoS Biol. 2020; 18(11):e3000953. https://doi.org/10.1371/journal.pbio.3000953.
2. Georgadaki K, Khoury N, Spandidos DA, Zoumpourlis V. The molecular basis of fertilization (Review). Int J Mol Med. 2016; 38(4):979-986. https://doi.org/10.3892/ijmm.2016.2723.
3. Klinovska K, Sebkova N, Dvorakova-Hortova K. Sperm-egg fusion: A molecular enigma of mammalian reproduction. Int J Mol Sci. 2014; 15(6):10652-10668. https://doi.org/10.3390/ijms150610652.
4. Tosti E, Menezo Y. Gamete activation: Basic knowledge and clinical applications. Hum Reprod Update. 2016; 22(4):420-439. https://doi.org/10.1093/humupd/dmw014.
5. Trebichalska Z, Holubcova Z. Perfect date-the review of current research into molecular bases of mammalian fertilization. J Assist Reprod Genet. 2020; 37(2):243-256. https://doi.org/10.1007/s10815-019-01679-4.
6. Breitbart H, Cohen G, Rubinstein S. Role of actin cytoskeleton in mammalian sperm capacitation and the acrosome reaction. Reproduction. 2005; 129(3):263-268. https://doi.org/10.1530/rep.1.00269.
7. Brener E, Rubinstein S, Cohen G, Shternall K, Rivlin J, Breitbart H. Remodeling of the actin cytoskeleton during mammalian sperm capacitation and acrosome reaction. Biol Reprod. 2003; 68(3):837-845. https://doi.org/10.1095/biolreprod.102.009233.

8. Griswold MD. Spermatogenesis: The Commitment to Meiosis. Physiol Rev. 2016; 96(1):1-17. https://doi.org/10.1152/physrev.00013.2015.
9. Lie PP, Mruk DD, Lee WM, Cheng CY. Cytoskeletal dynamics and spermatogenesis. Philos Trans R Soc Lond B Biol Sci. 2010; 365(1546):1581-1592. https://doi.org/10.1098/rstb.2009.0261.
10. Rathke C, Baarends WM, Awe S, Renkawitz-Pohl R. Chromatin dynamics during spermiogenesis. Biochim Biophys Acta. 2014; 1839(3):155-168. https://doi.org/10.1016/j.bbagrm.2013.08.004.
11. Staub C, Johnson L. Review: Spermatogenesis in the bull. Animal. 2018; 12(s1):s27-s35. https://doi.org/10.1017/S1751731118000435.
12. Teves ME, Roldan ERS, Krapf D, Strauss JF, III, Bhagat V, Sapao P. Sperm Differentiation: The Role of Trafficking of Proteins. Int J Mol Sci. 2020; 21(10). https://doi.org/10.3390/ijms21103702.
13. Xiao X, Mruk DD, Wong CKC, Cheng CY. Germ cell transport across the seminiferous epithelium during spermatogenesis. Physiology (Bethesda). 2014; 29(4):286-298. https://doi.org/10.1152/physiol.00001.2014.
14. Foster JA, Gerton GL. The Acrosomal Matrix. Adv Anat Embryol Cell Biol. 2016; 220:15-33. https://doi.org/10.1007/978-3-319-30567-7_2.
15. Hirohashi N, Yanagimachi R. Sperm acrosome reaction: Its site and role in fertilization. Biol Reprod. 2018; 99(1):127-133. https://doi.org/10.1093/biolre/ioy045.
16. Berruti G, Paiardi C. Acrosome biogenesis: Revisiting old questions to yield new insights. Spermatogenesis. 2011; 1(2):95-98. https://doi.org/10.4161/spmg.1.2.16820.
17. Fujihara Y, Satouh Y, Inoue N, Isotani A, Ikawa M, Okabe M. SPACA1-deficient male mice are infertile with abnormally shaped sperm heads reminiscent of globozoospermia. Development. 2012; 139(19):3583-3589. https://doi.org/10.1242/dev.081778.
18. Lin YN, Roy A, Yan W, Burns KH, Matzuk MM. Loss of zona pellucida binding proteins in the acrosomal matrix disrupts acrosome biogenesis and sperm morphogenesis. Mol Cell Biol. 2007; 27(19):6794-6805. https://doi.org/10.1128/MCB.01029-07.
19. Miyazaki T, Mori M, Yoshida CA, Ito C, Yamatoya K, Moriishi T, *et al*. Galnt3 deficiency disrupts acrosome formation and leads to oligoasthenoteratozoospermia. Histochem Cell Biol. 2013; 139(2):339-354. https://doi.org/10.1007/s00418-012-1031-3.
20. Pierre V, Martinez G, Coutton C, Delaroche J, Yassine S, Novella C, *et al*. Absence of Dpy19l2, a new inner nuclear membrane protein, causes globozoospermia in mice by preventing the anchoring of the acrosome to the nucleus. Development. 2012; 139(16):2955-2965. https://doi.org/10.1242/dev.077982.
21. Xiao N, Kam C, Shen C, Jin W, Wang J, Lee KM, *et al*. PICK1 deficiency causes male infertility in mice by disrupting acrosome formation. J Clin Invest. 2009; 119(4):802-812. https://doi.org/10.1172/JCI36230.
22. Paiardi C, Pasini ME, Gioria M, Berruti G. Failure of acrosome formation and globozoospermia in the wobbler mouse, a Vps54 spontaneous recessive mutant. Spermatogenesis. 2011; 1(1):52-62. https://doi.org/10.4161/spmg.1.1.14698.
23. Schmitt-John T, Drepper C, Mussmann A, Hahn P, Kuhlmann M, Thiel C, *et al*. Mutation of Vps54 causes motor neuron disease and defective spermiogenesis in the wobbler mouse. Nat Genet. 2005; 37(11):1213-1215. https://doi.org/10.1038/ng1661.
24. Haddad M, Stewart J, Xie P, Cheung S, Trout A, Keating D, *et al*. Thoughts on the popularity of ICSI. J Assist Reprod Genet. 2021; 38(1):101-123. https://doi.org/10.1007/s10815-020-01987-0.
25. Neri QV, Lee B, Rosenwaks Z, Machaca K, Palermo GD. Understanding fertilization through intracytoplasmic sperm injection (ICSI). Cell Calcium. 2014; 55(1):24-37. https://doi.org/10.1016/j.ceca.2013.10.006.
26. Tavalaee M, Nomikos M, Lai FA, Nasr-Esfahani MH. Expression of sperm PLCzeta and clinical outcomes of ICSI-AOA in men affected by globozoospermia due to DPY19L2 deletion. Reprod Biomed Online. 2018; 36(3):348-355. https://doi.org/10.1016/j.rbmo.2017.12.013.
27. Khawar MB, Gao H, Li W. Mechanism of Acrosome Biogenesis in Mammals. Front Cell Dev Biol. 2019; 7:195. https://doi.org/10.3389/fcell.2019.00195.
28. Nasr-Esfahani MH, Razavi S, Javdan Z, Tavalaee M. Artificial oocyte activation in severe teratozoospermia undergoing intracytoplasmic sperm injection. Fertil Steril. 2008; 90(6):2231-2237. https://doi.org/10.1016/j.fertnstert.2007.10.047.
29. Chen SR, Batool A, Wang YQ, Hao XX, Chang CS, Cheng CY, *et al*. The control of male fertility by spermatid-specific factors: searching for contraceptive targets from spermatozoon's head to tail. Cell Death Dis. 2016; 7(11):e2472. https://doi.org/10.1038/cddis.2016.344.
30. Suri A. Sperm-based contraceptive vaccines: current status, merits and development. Expert Rev Mol Med. 2005; 7(18):1-16. https://doi.org/10.1017/S1462399405009877.
31. Kaur K, Prabha V. Immunocontraceptives: New approaches to fertility control. Biomed Res Int. 2014; 2014:868196. https://doi.org/10.1155/2014/868196.
32. Sree S, Radhakrishnan K, Indu S, Kumar PG. Dramatic changes in 67 miRNAs during initiation of first wave of spermatogenesis in Mus musculus testis: Global regulatory

insights generated by miRNA-mRNA network analysis. Biol Reprod. 2014; 91(3):69. https://doi.org/10.1095/biolreprod.114.119305.
33. Tsuji-Hosokawa A, Kashimada K, Kato T, Ogawa Y, Nomura R, Takasawa K, *et al*. Peptidyl arginine deiminase 2 (Padi2) is expressed in Sertoli cells in a specific manner and regulated by SOX9 during testicular development. Sci Rep. 2018; 8(1):13263. https://doi.org/10.1038/s41598-018-31376-8.
34. Alghamdi M, Al Ghamdi KA, Khan RH, Uversky VN, Redwan EM. An interplay of structure and intrinsic disorder in the functionality of peptidylarginine deiminases, a family of key autoimmunity-related enzymes. Cell Mol Life Sci. 2019; 76(23):4635-4662. https://doi.org/10.1007/s00018-019-03237-8.
35. Rogers GE, Harding HW, Llewellyn-Smith IJ. The origin of citrulline-containing proteins in the hair follicle and the chemical nature of trichohyalin, an intracellular precursor. Biochim Biophys Acta. 1977; 495(1):159-175. https://doi.org/10.1016/0005-2795(77)90250-1.
36. Witalison EE, Thompson PR, Hofseth LJ. Protein Arginine Deiminases and Associated Citrullination: Physiological Functions and Diseases Associated with Dysregulation. Curr Drug Targets. 2015; 16(7):700-710. https://doi.org/10.2174/1389450116666150202160954.
37. Alghamdi M, Alasmari D, Assiri A, Mattar E, Aljaddawi AA, Alattas SG, *et al*. An Overview of the Intrinsic Role of Citrullination in Autoimmune Disorders. J Immunol Res. 2019;2019:7592851.https://doi.org/10.1155/2019/7592851.
38. Nagata S, Senshu T. Peptidylarginine deiminase in rat and mouse hemopoietic cells. Experientia. 1990; 46(1):72-74. https://doi.org/10.1007/BF01955420.
39. Rus'd AA, Ikejiri Y, Ono H, Yonekawa T, Shiraiwa M, Kawada A, *et al*. Molecular cloning of cDNAs of mouse peptidylarginine deiminase type I, type III and type IV, and the expression pattern of type I in mouse. Eur J Biochem. 1999; 259(3):660-669. https://doi.org/10.1046/j.1432-1327.1999.00083.x.
40. Urano Y, Watanabe K, Sakaki A, Arase S, Watanabe Y, Shigemi F, *et al*. Immunohistochemical demonstration of peptidylarginine deiminase in human sweat glands. Am J Dermatopathol. 1990; 12(3):249-255. https://doi.org/10.1097/00000372-199006000-00005.
41. `Wang S, Wang Y. Peptidylarginine deiminases in citrullination, gene regulation, health and pathogenesis. Biochim Biophys Acta. 2013; 1829(10):1126-135. https://doi.org/10.1016/j.bbagrm.2013.07.003.
42. Watanabe K, Akiyama K, Hikichi K, Ohtsuka R, Okuyama A, Senshu T. Combined biochemical and immunochemical comparison of peptidylarginine deiminases present in various tissues. Biochim Biophys Acta. 1988; 966(3):375-383. https://doi.org/10.1016/0304-4165(88)90088-8.
43. Watanabe K, Senshu T. Isolation and characterization of cDNA clones encoding rat skeletal muscle peptidylarginine deiminase. J Biol Chem. 1989; 264(26):15255-15260. https://doi.org/10.1016/S0021-9258(19)84818-4.
44. van Beers JJ, Zendman AJ, Raijmakers R, Stammen-Vogelzangs J, Pruijn GJ. Peptidylarginine deiminase expression and activity in PAD2 knock-out and PAD4-low mice. Biochimie. 2013; 95(2):299-308. https://doi.org/10.1016/j.biochi.2012.09.029.
45. Falcao AM, Meijer M, Scaglione A, Rinwa P, Agirre E, Liang J, *et al*. PAD2-Mediated Citrullination Contributes to Efficient Oligodendrocyte Differentiation and Myelination. Cell Rep. 2019; 27(4):1090-1102 e10. https://doi.org/10.1016/j.celrep.2019.03.108.
46. Assohou-Luty C, Raijmakers R, Benckhuijsen WE, Stammen-Vogelzangs J, de Ru A, van Veelen PA, *et al*. The human peptidylarginine deiminases type 2 and type 4 have distinct substrate specificities. Biochim Biophys Acta. 2014; 1844(4):829-836. https://doi.org/10.1016/j.bbapap.2014.02.019.
47. Cantarino N, Musulen E, Valero V, Peinado MA, Perucho M, Moreno V, *et al*. Downregulation of the Deiminase PADI2 Is an Early Event in Colorectal Carcinogenesis and Indicates Poor Prognosis. Mol Cancer Res. 2016; 14(9):841-848. https://doi.org/10.1158/1541-7786.MCR-16-0034.
48. Kanno T, Kawada A, Yamanouchi J, Yosida-Noro C, Yoshiki A, Shiraiwa M, *et al*. Human peptidylarginine deiminase type III: Molecular cloning and nucleotide sequence of the cDNA, properties of the recombinant enzyme, and immunohistochemical localization in human skin. J Invest Dermatol. 2000; 115(5):813-823. https://doi.org/10.1046/j.1523-1747.2000.00131.x.
49. Christophorou MA, Castelo-Branco G, Halley-Stott RP, Oliveira CS, Loos R, Radzisheuskaya A, *et al*. Citrullination regulates pluripotency and histone H1 binding to chromatin. Nature. 2014; 507(7490):104-108. https://doi.org/10.1038/nature12942.
50. Beato M, Sharma P. Peptidyl Arginine Deiminase 2 (PADI2)-Mediated Arginine Citrullination Modulates Transcription in Cancer. Int J Mol Sci. 2020; 21(4). https://doi.org/10.3390/ijms21041351.
51. Khajavi M, Zhou Y, Birsner AE, Bazinet L, Rosa Di Sant A, Schiffer AJ, *et al*. Identification of Padi2 as a novel angiogenesis-regulating gene by genome association studies in mice. PLoS Genet. 2017; 13(6):e1006848. https://doi.org/10.1371/journal.pgen.1006848.
52. Zhou Y, Mittereder N, Sims GP. Perspective on Protein Arginine Deiminase Activity-Bicarbonate is a pH-Independent Regulator of Citrullination.

Front Immunol. 2018; 9:34. https://doi.org/10.3389/fimmu.2018.00034.

53. Yu HC, Tung CH, Huang KY, Huang HB, Lu MC. The Essential Role of Peptidylarginine Deiminases 2 for Cytokines Secretion, Apoptosis, and Cell Adhesion in Macrophage. Int J Mol Sci. 2020; 21(16). https://doi.org/10.3390/ijms21165720.
54. Shimada N, Handa S, Uchida Y, Fukuda M, Maruyama N, Asaga H, *et al*. Developmental and age-related changes of peptidylarginine deiminase 2 in the mouse brain. J Neurosci Res. 2010; 88(4):798-806. https://doi.org/10.1002/jnr.22255.
55. Liu L, Zhang Z, Zhang G, Wang T, Ma Y, Guo W. Down-regulation of PADI2 prevents proliferation and epithelial-mesenchymal transition in ovarian cancer through inhibiting JAK2/STAT3 pathway in vitro and in vivo, alone or in combination with Olaparib. J Transl Med. 2020; 18(1):357. https://doi.org/10.1186/s12967-020-02528-0.
56. Khan SA, Edwards BS, Muth A, Thompson PR, Cherrington BD, Navratil AM. GnRH Stimulates Peptidylarginine Deiminase Catalyzed Histone Citrullination in Gonadotrope Cells. Mol Endocrinol. 2016; 30(10):1081-1091. https://doi.org/10.1210/me.2016-1085.
57. Kan R, Jin M, Subramanian V, Causey CP, Thompson PR, Coonrod SA. Potential role for PADI-mediated histone citrullination in preimplantation development. BMC Dev Biol. 2012; 12:19. https://doi.org/10.1186/1471-213X-12-19.
58. Horibata S, Rogers KE, Sadegh D, Anguish LJ, McElwee JL, Shah P, *et al*. Role of peptidylarginine deiminase 2 (PAD2) in mammary carcinoma cell migration. BMC Cancer. 2017; 17(1):378. https://doi.org/10.1186/s12885-017-3354-x.
59. Liu DY, Garrett C, Baker HW. Acrosome-reacted human sperm in insemination medium do not bind to the zona pellucida of human oocytes. Int J Androl. 2006; 29(4):475-481. https://doi.org/10.1111/j.1365-2605.2006.00681.x.
60. Chang X, Xia Y, Pan J, Meng Q, Zhao Y, Yan X. PADI2 is significantly associated with rheumatoid arthritis. PLoS One. 2013; 8(12):e81259. https://doi.org/10.1371/journal.pone.0081259.
61. Cherrington BD, Zhang X, McElwee JL, Morency E, Anguish LJ, Coonrod SA. Potential role for PAD2 in gene regulation in breast cancer cells. PLoS One. 2012; 7(7):e41242. https://doi.org/10.1371/journal.pone.0041242.
62. Darrah E, Giles JT, Davis RL, Naik P, Wang H, Konig MF, *et al*. Autoantibodies to Peptidylarginine Deiminase 2 Are Associated With Less Severe Disease in Rheumatoid Arthritis. Front Immunol. 2018; 9:2696. https://doi.org/10.3389/fimmu.2018.02696.
63. Gao BS, Rong CS, Xu HM, Sun T, Hou J, Xu Y. Peptidyl Arginine Deiminase, Type II (PADI2) Is Involved in Urothelial Bladder Cancer. Pathol Oncol Res. 2020; 26(2):1279-1285. https://doi.org/10.1007/s12253-019-00687-0.
64. Guo W, Zheng Y, Xu B, Ma F, Li C, Zhang X, *et al*. Investigating the expression, effect and tumorigenic pathway of PADI2 in tumors. Onco Targets Ther. 2017; 10:1475-1485. https://doi.org/10.2147/OTT.S92389.
65. Wang H, Xu B, Zhang X, Zheng Y, Zhao Y, Chang X. PADI2 gene confers susceptibility to breast cancer and plays tumorigenic role via ACSL4, BINC3 and CA9 signaling. Cancer Cell Int. 2016; 16:61. https://doi.org/10.1186/s12935-016-0335-0.
66. Wang L, Song G, Zhang X, Feng T, Pan J, Chen W, *et al*. PADI2-Mediated Citrullination Promotes Prostate Cancer Progression. Cancer Res. 2017; 77(21):5755-5768. https://doi.org/10.1158/0008-5472.CAN-17-0150.
67. Mohanan S, Horibata S, Anguish LJ, Mukai C, Sams K, McElwee JL, *et al*. PAD2 over expression in transgenic mice augments malignancy and tumor-associated inflammation in chemically initiated skin tumors. Cell Tissue Res. 2017; 370(2):275-283. https://doi.org/10.1007/s00441-017-2669-x.
68. McElwee JL, Mohanan S, Horibata S, Sams KL, Anguish LJ, McLean D, *et al*. PAD2 over expression in transgenic mice promotes spontaneous skin neoplasia. Cancer Res. 2014; 74(21):6306-6317. https://doi.org/10.1158/0008-5472.CAN-14-0749.
69. Inagaki M, Takahara H, Nishi Y, Sugawara K, Sato C. Ca2+-dependent deimination-induced disassembly of intermediate filaments involves specific modification of the amino-terminal head domain. J Biol Chem. 1989; 264(30):18119-18127. https://doi.org/10.1016/S0021-9258(19)84685-9.
70. Saiki M, Watase M, Matsubayashi H, Hidaka Y. Recognition of the N-terminal histone H2A and H3 peptides by peptidylarginine deiminase IV. Protein Pept Lett. 2009; 16(9):1012-1016. https://doi.org/10.2174/092986609789055449.
71. Wang Y, Wysocka J, Sayegh J, Lee YH, Perlin JR, Leonelli L, *et al*. Human PAD4 regulates histone arginine methylation levels via demethylimination. Science. 2004; 306(5694):279-283. https://doi.org/10.1126/science.1101400.
72. Lai NS, Yu HC, Tung CH, Huang KY, Huang HB, Lu MC. Increased peptidylarginine deiminases expression during the macrophage differentiation and participated inflammatory responses. Arthritis Res Ther. 2019; 21(1):108. https://doi.org/10.1186/s13075-019-1896-9.
73. Liu Y, Lightfoot YL, Seto N, Carmona-Rivera C, Moore E, Goel R, *et al*. Peptidylarginine deiminases 2 and 4

modulate innate and adaptive immune responses in TLR-7-dependent lupus. JCI Insight. 2018; 3(23):e124729. https://doi.org/10.1172/jci.insight.124729.

74. Arif M, Kato T. Increased expression of PAD2 after repeated intracerebroventricular infusions of soluble Abeta(25-35) in the Alzheimer's disease model rat brain: effect of memantine. Cell Mol Biol Lett. 2009; 14(4):703-714. https://doi.org/10.2478/s11658-009-0029-x.
75. Tu R, Grover HM, Kotra LP. Peptidyl Arginine Deiminases and Neurodegenerative Diseases. Curr Med Chem. 2016; 23(2):104-114. https://doi.org/10.2174/0929867323666151118120710.
76. Edfors F, Danielsson F, Hallström BM, Käll L, Lundberg E, Pontén F, *et al*. Gene-specific correlation of RNA and protein levels in human cells and tissues. Mol Syst Biol. 2016; 12(10):883. https://doi.org/10.15252/msb.20167144.
77. Lin J, Amir A. Homeostasis of protein and mRNA concentrations in growing cells. Nat Commun. 2018; 9(1):4496. https://doi.org/10.1038/s41467-018-06714-z.
78. Maier T, Güell M, Serrano L. Correlation of mRNA and protein in complex biological samples. FEBS Lett. 2009; 583(24):3966-3973. https://doi.org/10.1016/j.febslet.2009.10.036.
79. Moritz CP, Mühlhaus T, Tenzer S, Schulenborg T, Friauf E. Poor transcript-protein correlation in the brain: negatively correlating gene products reveal neuronal polarity as a potential cause. J Neurochem. 2019; 149(5):582-604. https://doi.org/10.1111/jnc.14664.
80. Payne SH. The utility of protein and mRNA correlation. Trends Biochem Sci. 2015; 40(1):1-3. https://doi.org/10.1016/j.tibs.2014.10.010.
81. Schwanhäusser B, Busse D, Li N, Dittmar G, Schuchhardt J, Wolf J, *et al*. Global quantification of mammalian gene expression control. Nature. 2011; 473(7347):337-342. https://doi.org/10.1038/nature10098.
82. Siewert E, Müller-Esterl W, Starr R, Heinrich PC, Schaper F. Different protein turnover of interleukin-6-type cytokine signalling components. Eur J Biochem. 1999; 265(1):251-257. https://doi.org/10.1046/j.1432-1327.1999.00719.x.
83. Dong S, Kojima T, Shiraiwa M, Mechin MC, Chavanas S, Serre G, *et al*. Regulation of the expression of peptidylarginine deiminase type II gene (PADI2) in human keratinocytes involves Sp1 and Sp3 transcription factors. J Invest Dermatol. 2005; 124(5):1026-1033. https://doi.org/10.1111/j.0022-202X.2005.23690.x.
84. Chang HH, Liu GY, Dwivedi N, Sun B, Okamoto Y, Kinslow JD, *et al*. A molecular signature of preclinical rheumatoid arthritis triggered by dysregulated PTPN22. JCI Insight. 2016; 1(17):e90045. https://doi.org/10.1172/jci.insight.90045.
85. Sun B, Chang HH, Salinger A, Tomita B, Bawadekar M, Holmes CL, *et al*. Reciprocal regulation of Th2 and Th17 cells by PAD2-mediated citrullination. JCI Insight. 2019; 4(22). https://doi.org/10.1172/jci.insight.129687.
86. Zheng L, Nagar M, Maurais AJ, Slade DJ, Parelkar SS, Coonrod SA, *et al*. Calcium Regulates the Nuclear Localization of Protein Arginine Deiminase 2. Biochemistry. 2019; 58(27):3042-56. https://doi.org/10.1021/acs.biochem.9b00225.
87. Sharma P, Lioutas A, Fernandez-Fuentes N, Quilez J, Carbonell-Caballero J, Wright RHG, *et al*. Arginine Citrullination at the C-Terminal Domain Controls RNA Polymerase II Transcription. Mol Cell. 2019; 73(1):84-96 e7. https://doi.org/10.1016/j.molcel.2018.10.016.
88. Qu Y, Olsen JR, Yuan X, Cheng PF, Levesque MP, Brokstad KA, *et al*. Small molecule promotes β-catenin citrullination and inhibits Wnt signaling in cancer. Nat Chem Biol. 2018; 14(1):94-101. https://doi.org/10.1038/nchembio.2510.
89. Slade DJ, Subramanian V, Thompson PR. Pluripotency: citrullination unravels stem cells. Nat Chem Biol. 2014; 10(5):327-328. https://doi.org/10.1038/nchembio.1504.
90. Xiao S, Lu J, Sridhar B, Cao X, Yu P, Zhao T, *et al*. SMARCAD1 Contributes to the Regulation of Naive Pluripotency by Interacting with Histone Citrullination. Cell Rep. 2017; 18(13):3117-3128. https://doi.org/10.1016/j.celrep.2017.02.070.